

UNDERWATER SHOCKS FROM BLASTING

Charles E. Joachim and Charles R. Welch, PhD
U.S. Army Engineer Waterways Experiment Station
Vicksburg, MS 39180-6199

Abstract

Underwater blasting causes not only ground shock but water-shock. Underwater shock attenuates less with range from the explosive source than ground shock and has the potential for killing fish or marine mammals or for damaging marine structures. The collapse and subsequent oscillation of the gas cavity surrounding the detonation can sometimes produce a greater impulse than the initial shock wave from the detonation. The airblast from underwater detonations can range from nuisance levels to damaging levels.

Underwater shock has been studied for military purposes for decades. The shock phenomena are governed by the diverging waves from the explosive source, tensile reflections from the surface, and compression or tensile reflections from the bottom. Methods to measure the shock phenomena involving a very high-frequency response to monitor the short rise times (sometimes on the order of pico-seconds) of the waveforms, have been developed.

Water-shock, some of the other phenomena associated with underwater blasting, the use of bubble screens to mitigate water-shock, and the traditional methods used to measure the pressure fields produced by underwater detonations, are discussed.

Introduction

Extensive military research efforts to study water-shock wave propagation and the effects of underwater detonations began in the early stages of World War II. The purpose of these efforts and subsequent research was to evaluate the response of submerged or partially submerged targets, e.g., ship hulls, submarines, underwater storage facilities, dams, and levees, etc., to the effects of an underwater detonation. The military research effort developed water-shock measurement and prediction techniques that have direct application to civilian underwater construction projects. This paper describes criteria for predicting blast effects from detonations in water and instrumentation techniques for monitoring such effects. The work reported here relates in part to that done in preparation of an Engineer Technical Letter (Corps of Engineers 1991).

Water-Shock Characteristics

Water-shock generated by an underwater detonation of high explosives travels at a speed of about 1,520 m/sec for pressure levels less than 210 MPa (Cole 1948). In shallow water,

the disturbance is characterized by the arrival of four principal waves (Figure 1): (1) an exponentially decaying, direct wave from the explosive source, (2) a surface-relief wave (tensile image of the direct wave), (3) a bottom-reflected wave, and (4) a wave transmitted through the bottom materials and refracted back into the water (Miller, et al. 1971). The effect of these different waves on the resultant pressure history is shown schematically in Figure 2. The resultant pressure-time history is the time-phased superpositioning of the direct, surface relief, reflected, and refracted pressure wave at a point. For shot geometries where the water surface and bottom are far removed from the explosion source and measuring locations, the direct wave is predominant.

For TNT, the amplitude of the direct wave can be estimated from Figure 3 (Cole 1948), in which the abscissa is in units of scaled range ($R/Q^{1/3}$), where R is in metres and Q is the explosive mass in kilograms. The water-shock impulse (time integral of the pressure history) for the direct wave from a TNT explosive source can be estimated from the graph shown in Figure 4. The ordinate in Figure 4 is in units of "scaled" impulse ($I/Q^{1/3}$), where I is in kilopascals-sec. Table 1 provides approximate factors for converting the masses of several common explosives to an equivalent mass of TNT. If the actual value of the equivalent mass of TNT is unknown, an upper estimate value of 2.0 will cover most common explosives (i.e., 1 kilogram of explosive is equivalent to no more than 2 kilograms of TNT).

The approximate value of the water-shock (in kilopascals), as a function of time (t , in sec), for the direct wave is described in Cole (1948) as:

$$P(t) = P_m e^{-\left(\frac{t - t_a}{\theta}\right)} \quad (1)$$

Where P_m , the peak pressure (in kPa) is

$$P_m = 52,400 (\lambda)^{-1.13} \quad (2)$$

θ , a time constant (in sec), is

$$\theta = 9.2 \times 10^{-5} Q^{1/3} (\lambda)^{0.18} \quad (3)$$

t_a , the shock arrival time (in sec) at the point of interest, is

$$t_a = R/1,524$$

and λ is the scaled range (in metres/ $Q^{1/3}$), where Q is the explosive mass (TNT equivalent (in kilograms)). The water-shock impulse at a scaled range of λ is

$$I(t) = 5.76 \times Q^{1/3} (\lambda)^{0.89} \quad (4)$$

The effect of the relief wave on the direct signal will be to shorten abruptly the duration of the pressure history seen at the point of interest. The effect of the bottom-reflected and bottom transmitted waves, for most bottom materials, will be to increase the pressure history duration.

Approximate upper-bound estimates for the peak pressures and impulses generated by the

presence of all four of these wave components is shown in Figures 3 and 4. Upper-bound limits of pressure and impulse can also be approximated by multiplying the value obtained from Equation 2 by 2.0, and that obtained from Equation 4 by 2.5 (from Miller, et al. 1971). Note that, because of the interaction of the direct wave with the surface-relief wave, actual peak pressures and impulses for shallow-water explosions can be a factor of 10 less than those given by Equations 2 and 4. Since variations in water depth can strongly affect the water-shock levels produced, especially at long ranges from a detonation, it is important to monitor the actual pressure and impulses generated by the explosive activities.

Significant secondary pressure pulsations can be caused by the rapid, repeated collapse and expansion of the explosion gas bubble in deep water. The peak pressures produced by these pulsations are less than 20 percent of the direct pulse. However, because the pulsations are of much longer duration, their associated impulse can be a factor of 4 larger than the impulse associated with the direct wave (Cole 1948).

Water-shock levels can be significantly reduced by the use of bubble screens between the area to be protected and the explosive source. This mechanism has been studied to prevent fish kills and structural damage to nearby marine structures (Strange 1963, Keevin et al., 1991). Reductions of peak pressures by a factor of 5 have been observed. The reduction mechanism appears to be two-fold: (1) the initial part of the direct wave is strongly attenuated by the bubble screen, and (2) the remaining portion of the direct wave is slowed down so that the surface relief wave can catch up and reduce the effect of the direct wave.

Care must be taken to avoid nuisance damage from airblast generated by the detonation of a high-explosive charge in shallow water. Figure 5 (from Swisdak 1975) provides isopressure contours of the airblast generated by underwater explosions as a function of scaled depth ($D/Q^{1/3}$), scaled range ($R/Q^{1/3}$), and at a constant scaled height above the water surface of $0.10 \text{ m/kg}^{1/3}$. In all cases, the charge should first be converted to its TNT equivalency before scaling. The airblast data are available only before scaling. Because of the scatter in the airblast data used in constructing the isopressure contours, the contours are considered accurate only within plus or minus 30 percent. Table 2 (Johnson 1971) provides anticipated damage levels caused by airblast at various overpressure levels.

The water plume created by an underwater explosion can be quite destructive to overhead structures. The water plume is one mechanism recommended for military use in bridge demolition (Armstrong 1979). Special attention must be paid to this risk when overhead structures exist in the vicinity of underwater detonations.

Water-Shock Monitoring Equipment

Water-shock pressures at a point of measurement are equal in all directions (i.e., they are hydrodynamic). Thus the orientation of a water-shock gage is not important. The tourmaline crystal pressure gage is the preferred transducer for measuring water-shock pressure because of its proven reliability and accuracy, ease of use, high-frequency response, and low sensitivity to temperature effects (Cole 1948, Tussing 1982).

Tourmaline is piezoelectric, which enables it to convert pressure (force per unit area) to electric energy. It should be noted, however, that piezoelectric crystals are not able to detect static or very slow changing pressure levels.

Tourmaline crystal water-shock gages can be manufactured, or purchased commercially (e.g., PCB Piezotronics, Inc.). In all cases, the tourmaline must be encapsulated in an electrical insulating material to prevent the generated charge from bleeding off into the surrounding water. The encapsulating material should have an acoustic impedance (sound speed times density) as close as possible to water to minimize distortion of the pressure measurements. It is extremely important that the encapsulating material have a high dielectric constant and does not generate a charge when stressed. This would cause errors in the measurements. One method of construction which satisfies these requirements is to use a tygon or PVC boot filled with silicone oil (Figure 6) to encapsulate the tourmaline crystal (Tussing 1982).

The amount of charge developed by the gage, or the gage sensitivity, is directly proportional to the area of the tourmaline crystal being loaded. Tourmaline crystals used for water-shock measurements range from 3.2 to 50.8 mm in diameter. The diameter of the crystal selected is a compromise between choosing one that is physically small (gage transit time small relative to shock duration) but large enough to provide adequate electrical output for the recording system. A rule of thumb to estimate the error in the peak measured pressure due to the gage transit time T_d , for θ/T_d ratios >5 is given by (from Tussing 1982):

$$\text{percent peak error} = \frac{0.5T_d}{\theta} \times 100\% \quad (5)$$

The equation applies to cases in which the amplitude of the direct wave is not affected by surface-relief or bottom-reflected waves during the engulfment time of the gage. The effect of the error is to cause the measured peak pressures to be below the actual peak pressures. The engulfment time, T_d , of the gage is the gage diameter divided by the wave velocity in water (1520 m/sec). Theta is given by equation 3. For gages using silicone fluid as the encapsulating material around the gage, the calculated transit time should be increased by 50 percent (Tussing 1982).

Tourmaline crystals are often stacked together and connected in a parallel network to increase the sensitivity of the gage without increasing the diameter of the gage (Figure 6). Typical gage sensitivities range from 0.36 picocoulombs per kPa for a 6.4-mm diameter doublet crystal (two crystals) gage, to 13 picocoulombs per kPa for an eight-stack pile of 3.2-mm diameter crystals (Cole 1948).

Most water-shock gages including those presently in use by the U.S. Navy, employ tourmaline gages connected by coaxial cable to the associated signal conditioning, amplifying, and recording systems. Tourmaline water-shock gages employed in this manner

are high-impedance devices. As such, they are not compatible with normal low-impedance instrumentation amplifier circuits. To achieve compatibility, the high-impedance gage is coupled to the low-impedance amplifier through a charge amplifier or impedance converter. These are available from several commercial sources. The charge amplifier or impedance converter is placed as near as possible to the gage to reduce the length of the connecting cable. However, the length of the connecting cable can be several tens of metres long for the impedance converter and possibly 300 to 600 metres long in the case of the charge amplifier.

Water-shock measurements of this type are particularly susceptible to noise sources: that induced by low-circuit resistance to ground (gage and cable in contact with the water), and water shock-induced cable noise. Care must be taken to ensure that the electrical resistance between the water-shock transducer circuit (gage and connecting cable) is as high as possible to limit system- background noise. Electrical resistance to ground and across the tourmaline crystal should be 100 Megohms or greater. Circuits submersed in water with low resistance to ground, pick up stray electrical noise from the surroundings and are susceptible to noise from electrical energy given off by the detonation of the explosive charge. Leakage across the crystal produces drift in charge amplifiers and degrades low-frequency response in impedance converters.

Coaxial cables used to connect the tourmaline water-shock gages to the charge amplifier should be antimicrophonic or low noise cable. Standard coaxial cable generates electrical noise when subjected to the high-shock environment that exists in water near a detonation. Antimicrophonic coaxial cable has graphite between the outer shield and the inner insulator. This greatly reduces the amount of charge generated on the cable due to water-shock.

Figure 7 is an idealization of a tourmaline gage connected to a charge amplifier via a coaxial cable. The RC-time constant for the circuit is determined by the electrical resistance across the crystal in parallel with the input impedance of the charge amplifier, the combined capacitance of the crystal, and the coaxial cable in parallel, and cable compensation networks. The RC-time constant is the time that it takes for the voltage from the charge due to a suddenly applied hydrostatic pressure to fall to $1/e = 0.368$ of its maximum value. Thus, the larger the RC-time constant, the better the low-frequency response of the gage. RC-time constants of several seconds are possible with proper precautions (Cole 1948).

To determine the calibration factor, KA, in picocoulombs per kPa, for the tourmaline watershock gage, a dynamic pressure environment is desirable but not usually practical. The calibration method normally adopted, providing the RC-time constant of the gage and calibration circuit is sufficiently long, is to statically pressurize the gage to some desired pressure and then quickly release the pressure (Cole 1948).

An electrical calibration, which takes into account amplifier gain settings and other attributes of the electrical circuit that is connected to the gage, must also be performed. The standard technique is the Q-step calibration shown in Figure 8 (from Cole 1948). If a

voltage, V_s , is applied to the capacitor, C_s , then the resulting voltage, V_c , at the open end of the circuit is given by:

$$V_c = \frac{C_s V_s}{C + C_s + C_s} \quad (6)$$

where C is the capacitance of the cable and C_0 is the capacitance of the gage. The voltage, V_p , produced by an applied pressure P to the gage is then given by:

$$V_p = P \left(\frac{V_c (KA)}{C_s V_s} \right) \quad (7)$$

The Q-step method is not used to provide an electrical calibration of the transducer circuit when using tourmaline crystal gages with the in-line impedance converters. Instead, the manufacturer provides a calibration constant, in terms of kPa per volt of gage output, which takes into account the characteristics of the tourmaline crystal and the charge amplifier (assuming proper power is provided to the in-line amplifier). For this situation, a known voltage step is normally applied to the input to the recording system and used as a calibration step or scale. A signal generator, available from the manufacturer, is used to simulate the water-shock gage and validate the signal amplifying system. To provide proper circuit damping, a series resistor is used between the gage and the power supply.

Rise-times of 2 to 3 μ sec have been achieved with cable lengths of 300 m between gage and amplifier.

A potential problem that exists for very high-frequency, short-duration water-shock measurements is ringing or oscillation of the electrical signal in the coaxial cable. Circuit ringing manifests itself as oscillations in the signal output. Proper termination of both ends of the coaxial cable with capacitor/resistor networks, as shown in Figure 9, prevents this oscillation while still providing acceptable frequency response (from Cole 1948). If L is the total distributed inductance of the cable (i.e., the inductance per unit length times the total cable length) and C is the total distributed capacitance of the cable, then the surge resistance R_0 , is defined to be:

$$R_0 = \sqrt{L/C} \quad (8)$$

In Figure 9, R_1 and R_2 are made to be approximately equal to the surge resistance R_0 of the cable, and the capacitors C_1 and C_2 are equal to the distributed capacitance, C , of the cable.

Some commercial water-shock gages (e.g., PCB Piezotronics, Inc.) have in-line impedance converters built into the gage housing. This eliminates the need for low-noise cable, reduces the requirement for high impedance between the cable and the water, and eliminates the need for charge amplifiers. Such instruments are more convenient than the older circuits. They also usually do not have as good a low-frequency response as the tourmaline crystals connected via properly handled coaxial circuits to a charge amplifier. There appears, however, to be no intrinsic reason why the commercial gages could not be

configured to have longer RC-time constants.

Although high cable insulation (>100 Megohms) is not required for the commercial gages, care must be taken not to allow moisture contamination of the cable and the gage. If this occurs, then the recorded pressure histories will fall off more rapidly than the actual phenomena. Another symptom is the recording, during part of the pressure history, of apparent negative pressures below the combination of atmospheric and hydrostatic pressures of the overlying water.

Amplifier and recording systems selected to record water-shock pressures, for both the basic tourmaline crystal gage and the tourmaline crystal gage with in-line impedance matching circuit, should have sufficient sensitivity to provide a low signal-to-noise ratio for the recorded pressure-time history.

System frequency response is limited by the frequency response of the individual components of the system. Piezoelectric gages and properly terminated coaxial cables, in general, pass higher frequencies than amplifiers and recording systems. Therefore, care must be taken to ensure that the amplifiers and recording system have sufficient frequency response to reliably record the phenomena. The smaller the explosive charge or the closer the free surface of the water to the measurement, the shorter the duration of the water-shock pulse. For example, water-shock pressure measurements from a 4.5-kg TNT equivalent explosive charge in 1.2 m of water at a 9.9-m range show pressure durations of the initial pulse on the order of 20 μ sec (Henry and Welch, unpublished data). From a practical standpoint, instrumentation amplifiers with 5-percent down points of 50 to 100 kHz are readily available.

A variety of recording systems exists for storing the measured electrical records from watershock gages. FM magnetic-tape machines offer acceptable (80 kHz) frequency response and provide extended record times (minutes) so that the sequencing of tape machine turn-on and explosive charge detonation presents little problem. Digital transient recorders operating at a minimum of 500,000 samples per second, with 12-bit accuracy, offer better resolution than tape recorders as well as ease of data handling with computers. These systems, however, record for much less time (generally 16,000 to 256,000 data points, or 32 to 512 msec) than the tape machines, and the sequencing between charge detonation and data capture is more critical. Digital oscilloscopes often have lower data resolution (8-bit) but have higher frequency response (several mega samples per second) than the transient data recorders. Analog storage oscilloscopes, or analog oscilloscopes with photographic capture, provide frequency response into the 100's of MHz, but have much worse signal amplitude resolution than the digital recording systems. Similar to the digital recording systems, the sequencing of data capture is critical with the oscilloscopes.

Summary

This paper presents a discussion of water-shock and some of the phenomena associated with underwater blasting. Traditional methods used to measure the pressure fields

produced by underwater detonations and the use of bubble screens to mitigate water-shock and prevent damage to structures and aquatic life are also discussed.

Acknowledgment

We appreciate the cooperation of the authorities at the U.S. Army Engineer Waterways Experiment Station, and the Headquarters, U.S. Army Corps of Engineers that permitted us to prepare and present this paper for publication.

References

Armstrong, B. J., Jr., 1979, "Destruction of Bridge Decking with Explosion-Produced Water Plumes," Miscellaneous Paper SL-79-5, U.S. Army Engineer Waterways Experiment Station, Vicksburg, MS.

Cole, Robert H., 1948, "Underwater Explosions," Dover Publications, Inc., New York, NY.

Corps of Engineers, 1991, "Engineering and Design, Underwater Blast Monitoring," Engineer Technical Letter, ETL 1110-8-11(FR), U.S. Army Corps of Engineers, Washington, DC.

Johnson, Stanley M., 1971, "Explosive Excavation Technology," NCG TR 21, U.S. Army Engineer Nuclear Cratering Group, Livermore, CA.

Keevin, T. M., Hempen, G. L., Nico, L. G., and Schaeffer, D., 1991, "The Use of a Bubble Screen Curtain to Reduce Fish Mortality Resulting from Underwater Explosions," North American Journal of Fisheries Management.

Langefors, U., and Kihlstrom, B., 1978, "The Modern Technique of Rock Blasting," Halsted Press, Wiley, New York, NY.

Miller, L., Strange, J. N., and Pinkston, J. M., Jr., 1971, "Water Shock Reflection Properties of Various Bottom Materials - Final Report - Volume 1: Main Text," Technical Report 1-704, U.S. Army Engineer Waterways Experiment Station, Vicksburg, MS.

Petes, J., Miller, R., and McMullan, R., 1983, "Users Guide and History of ANFO as a Nuclear Weapons Effect Simulation Explosive," Defense Nuclear Agency, Washington, DC.

Strange, J. N., 1963, "The Attenuating Effects of a Bubble Screen on Underwater Shock," Miscellaneous Paper 2-553, U.S. Army Engineer Waterways Experiment Station, Vicksburg, MS.

Swisdak, Michael M., Jr., 1975, "Explosion Effects and Properties, Part 1 - Explosion Effects in Air," NSWC/NOL/TR 75- 116, White Oak Laboratory, Naval Surface Weapons

Center, White Oak, MD.

Tussing, Ronald B., 1982, "Accuracy and Response of Tourmaline Gages for Measurement of Underwater Explosion Phenomena," NSWC TR-82-294, Naval Surface Weapons Center, White Oak, MD.

Table 1 Approximate TNT Conversion Factor for Selected High Explosives	
Explosive	Approximate Conversion Factor by Weight for Pressure
TNT	1
Nitromethane	1.1 ¹
Pentalite	1.04 ²
ANFO	0.3-0.82 ³
C-4	1.37 ⁴
Ammonium Dynamite	0.7-0.9 ⁴
Gelatin Dynamite	0.7-0.8 ⁴
Nitroglycerin Dynamite	0.9 ⁴

¹ Hendry and Welch (unpublished data).

² Cole (1948).

³ Dependent on percent fuel oil: factors estimated based on energy content taken from Petes, et al, (1983).

⁴ Estimated based on airblast data and energy content (Swisdak 1975)

Table 2. Airblast Damage Criteria (Johnson 1971)	
Overpressure, (kPa)	Degree of Estimated Damage
0.200	Possible window damage, particularly to large store windows
0.303	Some damage to large plate glass windows can be expected
0.448	Some damage to average size windows can be expected
1.310	Extensive damage to windows; probably damage to average wooden doors
3.999	Most small casement windows smashed
>3.999	Structural damage possible

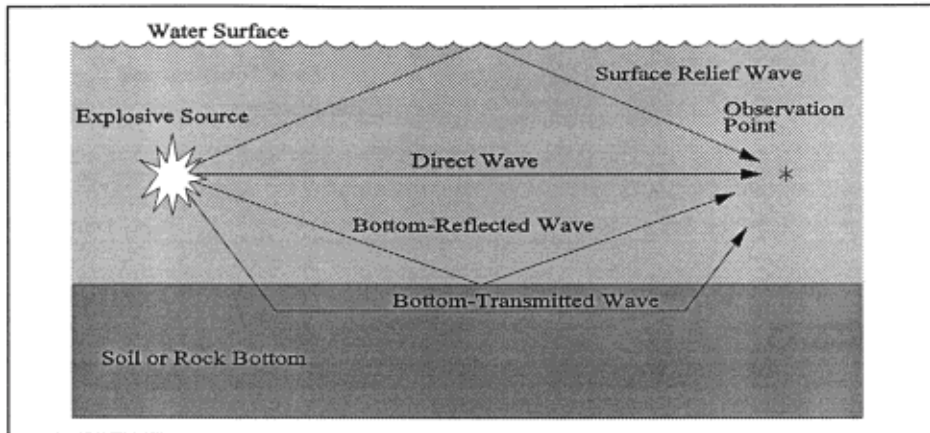


Figure 1. Four principal waves associated with shallow water explosions

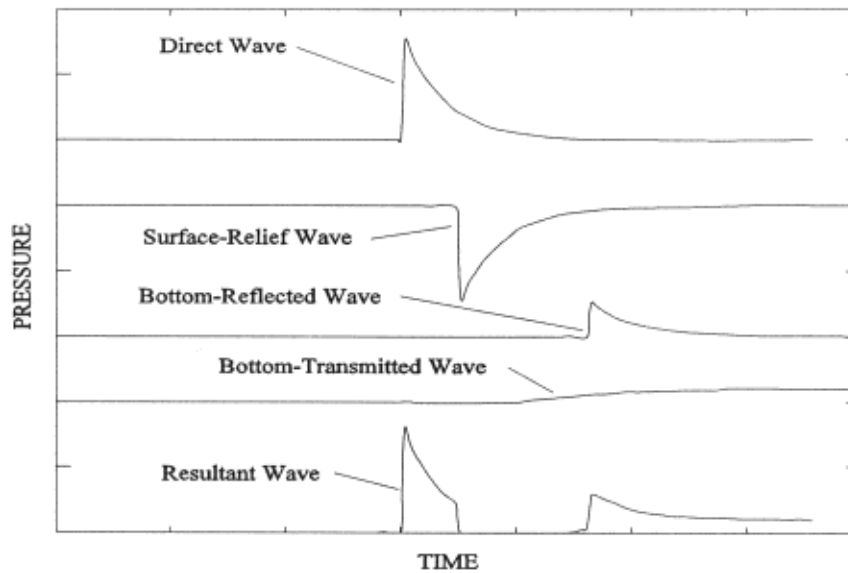


Figure 2. Effects of different wave components on the water-shock measured at a point.

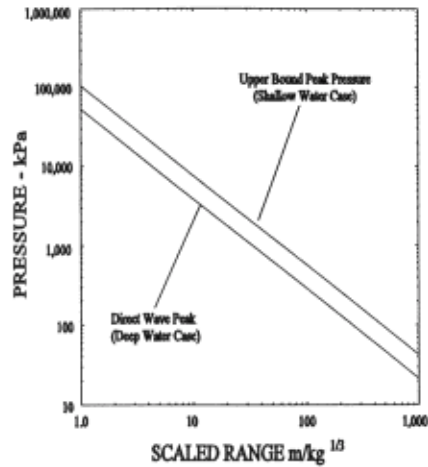


Figure 3. Peak pressure as a function of scaled range for the direct wave from a TNT explosion (from Cole 1948).

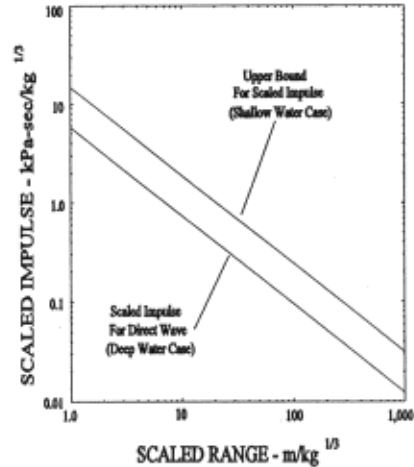


Figure 4. Scaled impulse from the direct wave from a TNT explosion (from Cole 1948).

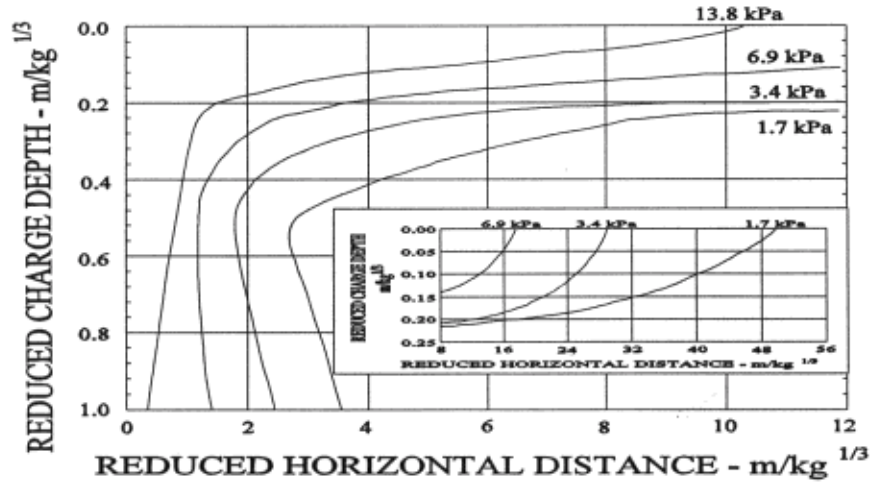


Figure 5. Airblast isopressure contours at a height of $0.1 m/kg^{1/3}$ above the water surface from TNT spheres fired at various scaled depths (from Swisdak 1975).

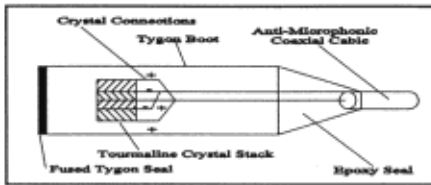


Figure 6. Four-stack tourmaline crystal water-shock pressure gage employing tygon boot filled with silicone oil.

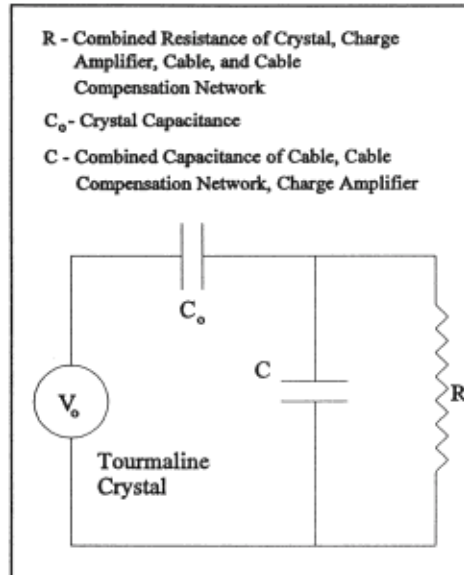


Figure 7. Idealization of circuit components which determine RC-time constant of tourmaline gage.

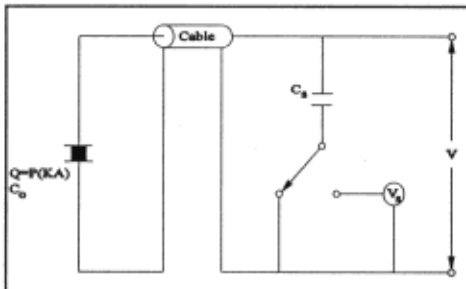


Figure 8. "Q-step" calibration circuit (from Cole 1948).

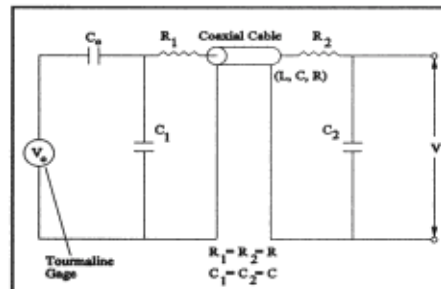


Figure 9. Schematic showing cable compensation network R_1 , R_2 , C_1 , and C_2 which minimizes circuit ringing (from Cole 1948).